NAVAL POSTGRADUATE SCHOOL

MONTEREY, CALIFORNIA

THESIS

DETECTION OF FREQUENCY-HOPPED SIGNALS EXPOSED TO NON-STATIONARY INTERFERENCE

by

Steven C. Layfield

December 2008

Thesis Advisor: Clark Robertson
Second Reader: Roberto Cristi

Approved for public release; distribution is unlimited

THIS PAGE INTENTIONALLY LEFT BLANK

1. AGENCY USE ONLY (*Leave blank*)	2. REPORT DATE December 2008	3. REPORT TYPE AND DATES COVERED Master's Thesis	
4. TITLE AND SUBTITLE: Detection Of Frequency-Hopped Signals Embedded in Non-Stationary Interference		**5. FUNDING NUMBERS**	
6. AUTHOR Steven C. Layfield			
7. PERFORMING ORGANIZATION NAME(S) AND ADDRESS(ES) Naval Postgraduate School Monterey, CA 93943-5000		**8.PERFORMING ORGANIZATION REPORT NUMBER**	
9. SPONSORING /MONITORING AGENCY NAME(S) AND ADDRESS(ES) N/A		**10. SPONSORING/MONITORING AGENCY REPORT NUMBER**	
11. SUPPLEMENTARY NOTES The views expressed in this thesis are those of the author and do not reflect the official policy or position of the Department of Defense or the U.S. Government.			
12a. DISTRIBUTION / AVAILABILITY STATEMENT Approved for public release; distribution is unlimited		**12b. DISTRIBUTION CODE** A	

13. ABSTRACT (maximum 200 words)

Frequency-hopped spread spectrum signals are widely used in military communications to help combat or suppress interference due to jamming, other users of the channel, and multipath propagation. Frequency-hopped signals may be difficult to detect when embedded in background noise. Previous research has demonstrated techniques for interference reduction and filtering frequency-hopped spread spectrum waveforms with minimum distortion when the frequency-hop rate is on the order of 1,000 hops per second and the waveform is embedded in stationary interference waveforms. The objective of this thesis was to apply previously developed interference reduction techniques to frequency-hopped signals that hop at a much lower rate in order to determine the efficacy and practicality of these techniques for hop rates as low as five frequency-hops per second when the signal-of-interest is embedded in non-stationary interference. The technique used in this thesis to detect the frequency-hopped signals-of-interest is based on exponential averaging in the frequency domain. This method averages a weighted datastream in realtime. Specific fast Fourier transform block sizes and exponential average weights produce good results if the signal-to-interference and the signal-to-noise ratios are not too small.

14. SUBJECT TERMS Noise-normalization, Detection, Estimation, Spread Spectrum, Frequency-Hopped, interference estimate, exponential average	15. NUMBER OF PAGES 57
	16. PRICE CODE

17. SECURITY CLASSIFICATION OF REPORT Unclassified	18. SECURITY CLASSIFICATION OF THIS PAGE Unclassified	19. SECURITY CLASSIFICATION OF ABSTRACT Unclassified	20. LIMITATION OF ABSTRACT UU

THIS PAGE INTENTIONALLY LEFT BLANK

DETECTION OF FREQUENCY-HOPPED SIGNALS EXPOSED TO NON-STATIONARY INTERFERENCE

Steven C. Layfield
Lieutenant, United States Navy
B.S., Southern Polytechnic State University, 2002

Submitted in partial fulfillment of the
requirements for the degree of

MASTER OF SCIENCE IN ELECTRICAL ENGINEERING

from the

**NAVAL POSTGRADUATE SCHOOL
December 2008**

Author: Steven C. Layfield

Approved by: R. Clark Robertson
                 Thesis Advisor

                 Roberto Cristi
                 Second Reader

                 Jeffrey B. Knorr
                 Chairman, Department of Electrical and Computer Engineering

THIS PAGE INTENTIONALLY LEFT BLANK

ABSTRACT

Frequency-hopped spread spectrum signals are widely used in military communications to help combat or suppress interference due to jamming, other users of the channel, and multipath propagation. Frequency-hopped signals may be difficult to detect when embedded in background noise. Previous research has demonstrated techniques for interference reduction and filtering frequency-hopped spread spectrum waveforms with minimum distortion when the frequency-hop rate is on the order of 1,000 hops per second and the waveform is embedded in stationary interference waveforms. The objective of this thesis was to apply previously developed interference reduction techniques to frequency-hopped signals that hop at a much lower rate in order to determine the efficacy and practicality of these techniques for hop rates as low as five frequency-hops per second when the signal-of-interest is embedded in non-stationary interference.

The technique used in this thesis to detect the frequency-hopped signals of interest is based on exponential averaging in the frequency domain. This method averages a weighted datastream in realtime. Specific fast Fourier transform block sizes and exponential average weights produce good results if the signal-to-interference and the signal-to-noise ratios are not too small.

THIS PAGE INTENTIONALLY LEFT BLANK

TABLE OF CONTENTS

THIS PAGE INTENTIONALLY LEFT BLANK

LIST OF FIGURES

LIST OF TABLES

THIS PAGE INTENTIONALLY LEFT BLANK

EXECUTIVE SUMMARY

Recovery techniques for a high frequency/frequency-hopped (HF/FH) test signal embedded in a real-world environment were investigated in this thesis. The HF/FH test signal is a FH single-sideband suppressed-carrier signal. Frequency-hopping is used in military communications to help combat or suppress interference due to jamming, other users of the channel, and multipath propagation. The HF/FH test signal can be difficult to detect when embedded in background noise. The objective of this thesis was to modify previously derived theoretical methods used to detect FH signals with high hop rates exposed to stationary noise to the HF/FH test signal embedded in a real-world, non-stationary, and multiple-access environment.

The first step in recovering the HF/FH test signal was to determine the frequency-domain representation of the interference signal by exponentially averaging. The HF/FH test signal and the interference it was embedded in was broken into smaller data segments (*N*-point windows), and the magnitude of each FFT window was computed. These windows were used to form an interference estimate which ideally does not contain the HF/FH test signal. The number of frames used for each estimate, the weight applied to each frame, and the FFT size are the variables involved in generating the interference estimate. A block diagram of the exponential averaging technique to estimate the interference spectrum is shown in the following figure:
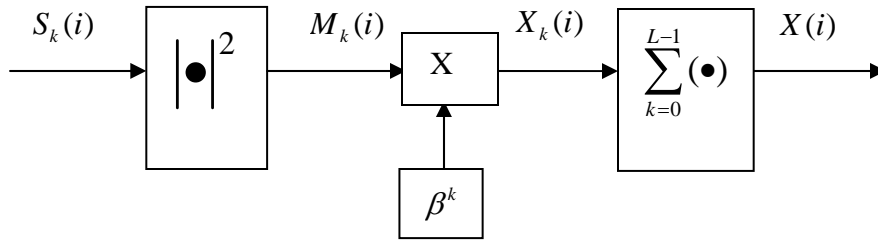
where *X(i)* is the spectral interference estimate, β is a weight factor between 0 and 1, $M_k(i)$ is magnitude squared of the FFT of the current *N*-point window, $S_k(i)$ is the FFT of one data block, and $k = 0,1,2,\ldots,L-1$ where L is the number *N*-point of segments that the data is separated into. The parameters were determined using trial-and-error. The

success of the exponential averaging algorithm depends on choosing the correct parameters. A FFT window size that is too large generates an estimate from a small number of windows and does not average out all of the HF/FH signal components. A FFT window size that is too small generates an estimate from a large number of windows, which averages out the entire HF/FH signal but also some of the interference. In order to obtain a good estimate of the interference, a balance between too large and too small of a FFT window size is imperative. Another influential parameter is the weight factor of the exponential averaging algorithm. The weight factor defines how much early-time elements in the exponential average are weighted. A large weight factor results in over-emphasizing early-time frames in the overall sequence. This does not allow the early-time frequency hops in the sequence to diminish rapidly enough because each new frame only contributes a small amount to the interference estimate. In this case, not all of the HF/FH signal components are extracted. A small weight factor results in over-emphasizing late-time frequency hops in the time sequence and magnifies the current contribution to the estimate. Consequently, choosing the right weight factor is imperative in obtaining a good representation of the interference. For a 16,777,216-point window, a FFT of 2^{16} points and a weight factor between 0.93 and 0.96 resulted in the best interference spectrum estimate.

The second step in recovering the HF/FH signal uses the interference estimate to extract the HF/FH signal through a type of normalization, either spectral division or spectral subtraction. Spectral division is a process that divides each frame of the received signal by the interference estimate. Frame-by-frame spectral subtraction subtracts a scaled version of the noise estimate from the composite signal. After normalization, the signal-of-interest is recovered. Spectral subtraction is the best recovery method when the signal-to-additive white Gaussian noise ratio (SNR) and signal-to-interference ratio (SIR) are relatively high, but when the SNR and SIR are both less than −4 dB, spectral division is a better approach. Certain FFT window sizes and weight factors resolve the HF/FH signal better than others. In order to obtain the best possible spectrum of the HF/FH signal, a balance between the two parameters must be achieved. In this thesis, trial-and-error was used to determine the balance.

The threshold of detection and processing were determined using a combination of different SNR and SIR. It was assumed that recovering $n-2$ frequency hops of an n-hop signal imply processing is possible and that recovering $n/2$ or more frequency hops implies detection is possible. For spectral division, a SIR of -4 dB and a SNR of -4 dB were determined to be the threshold for processing, and a SIR of -12 dB and a SNR of -4 dB were found to be the threshold for detection. For spectral subtraction, a SIR of -2 dB and a SNR of -8 dB were determined to be the threshold for processing, and a SIR of -4 dB and a SNR of -8 dB were found to be the threshold for detection.

This thesis demonstrated that the exponential averaging algorithm can be used to successfully form an interference estimate and subsequently detect HF/FH signals when the interference is non-stationary.

THIS PAGE INTENTIONALLY LEFT BLANK

ACKNOWLEDGMENTS

I thank God first and foremost for blessing me with the opportunity, support of my family and loved ones, and ability to accomplish such a challenging task.

I dedicate this work to my lovely wife, Melissa Layfield, and my wonderful daughter, Savannah Parker Layfield for their continuous and generous support in my educational and military career.

Also, I would like to extend my sincere appreciation to Professor Clark Robertson and Professor Roberto Cristi for their constant support, guidance, encouragement and patience in order to complete this work.

Finally, I am grateful to the United States Navy for giving me the opportunity to expand my educational horizons at Naval Postgraduate School.

THIS PAGE INTENTIONALLY LEFT BLANK

I. INTRODUCTION

A. OVERVIEW AND OBJECTIVE

Frequency-hopped spread spectrum (FH-SS) radios are widely used in foreign and domestic military communications due to the fact that they are less vulnerable to processing, detection, and jamming than conventional fixed frequency radios that are designed to transmit and receive on a single channel. Processing is defined as successful demodulation of the signal. Detection is the ability to determine the presence of signal energy in a frequency band of interest. Jamming is the deliberate disruption of communication by operating a transmitter (jammer) in the same frequency band as the desired signal [1]. Frequency-hopping can be an effective counter measure to each of these. Frequency-hopped spread spectrum signals help combat or suppress electronic warfare (EW) attacks by subdividing the available channel bandwidth into a large number of contiguous frequency slots. When the signal is embedded in background noise and transmitted at low power the signal can be very difficult to detect, much less process [2]. A high frequency, frequency-hopping (HF/FH) test signal is used for the analysis in this thesis.

Previous work proved that a digitally modulated FH-SS signal at a fast hop rate could be recovered by using an exponential averaging algorithm [3], [4]. This was done by first estimating the interference environment and then using this estimate to recover the signal-of-interest. Previous work used laboratory generated, digitally modulated, frequency-hopped signals and stationary interference signals with no noise [3]. The work in [3] was expanded by adding additive white Gaussian noise (AWGN) to the interference in [4]. This thesis extends the work in [3] and [4] by adapting the exponential average algorithm to recover a HF/FH test signal with a very low hop rate in a non-stationary interference environment. Furthermore, the exponential average algorithm is used to recover a non-digital signal, specifically, a single-side band, suppressed carrier waveform (SSB/SC).

B.   THESIS OUTLINE

This thesis contains four parts. Background information on the frequency-hopping test signal is described in Chapter II. In Chapter III, the interference signals that the HF/FH is exposed to and the signal processing that is required to obtain a composite signal consisting of both interference and the signal-of-interest is described. The recovery of the HF/FH signal is discussed in Chapter IV. A description of the effects of signal-to-AWGN ratio (SNR) and signal-to-interference ratio (SIR) on the ability to either detect or process the signal-of-interest is discussed in Chapter V. Conclusions and recommendations for further research are presented in the final chapter, Chapter VI.

II.   FREQUENCY-HOPPED TEST AND INTERFERENCE SIGNALS

The FH-SSB/SC test signal and the non-stationary interference signal are discussed in this chapter. MATLAB was used to process the signals.

A.   FREQUENCY-HOPPED SPREAD SPECTRUM SIGNAL-OF-INTEREST

The frequency-hopped spread spectrum signal-of-interest used in [3] and [4] was a frequency-hopped, minimum-shift keyed (FH/MSK) signal with a hop rate of 1,000 hops per second and a 5.8 MHz hop bandwidth. The frequency-hopped spread spectrum signal-of-interest used in this thesis is an HF signal and has a much slower hop rate of five hops per second and a much smaller hop band of 256 KHz. The HF/FH test signal uses single side-band, suppressed carrier (SSB/SC) modulation and was collected in a laboratory environment, providing a high-quality sample of the test signal. In this thesis, the HF/FH test signal is referred to as the laboratory data. A digital signal such as MSK has a characteristic spectrum as shown in Figure 1, and a SSB/SC signal has a spectrum as shown in Figure 2. The MSK spectrum is more uniform and more symmetric than the spectrum of the SSB/SC signal, and the SSB/SC signal, with its jagged characteristics, may be more easily mistaken as noise when the signal power is small. As shown in Figure 3 and Figure 4, the spectrum of a frequency-hopped signal, independent of the type of modulation, is easily distinguished from noise when the signal-to-noise interference ratio is not too small. The spectrum in Figure 3 as compared to the spectrum shown in Figure 4 is more obviously a signal; however, the frequency-hop band in Figure 4 is clearly visible above the noise floor. As the FH-SSB/SC shown in Figure 4 approaches the noise floor, the harder it becomes to distinguish it from the noise.
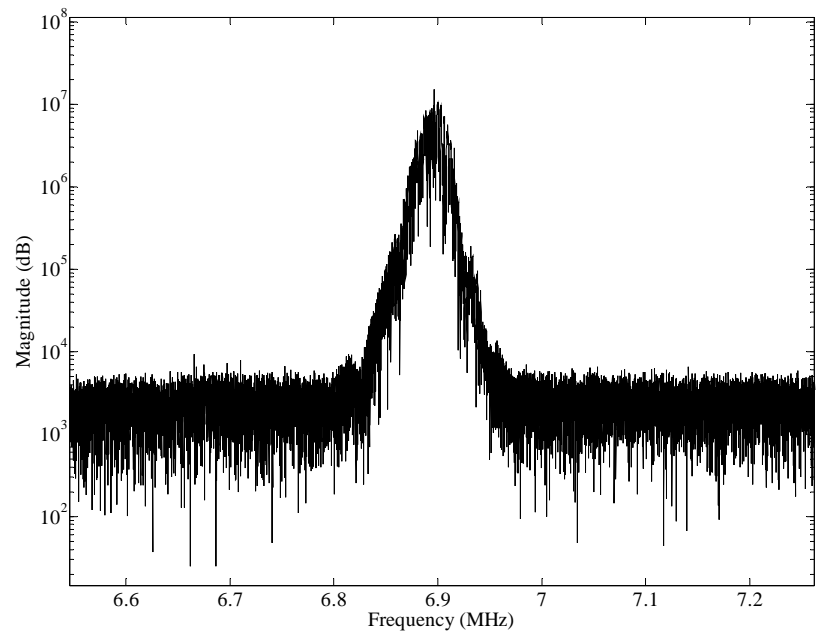
Figure 1.   Instantaneous spectrum of a MSK modulated signal [3].
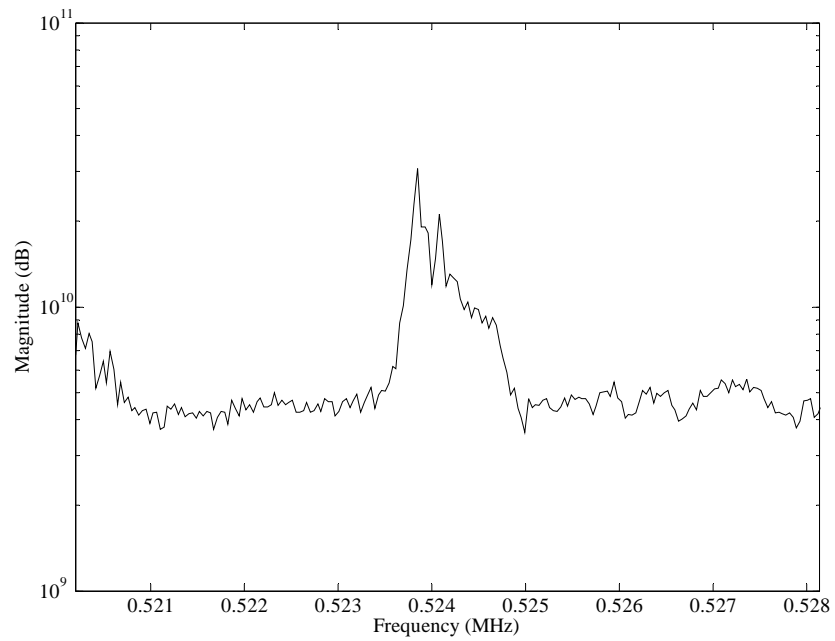

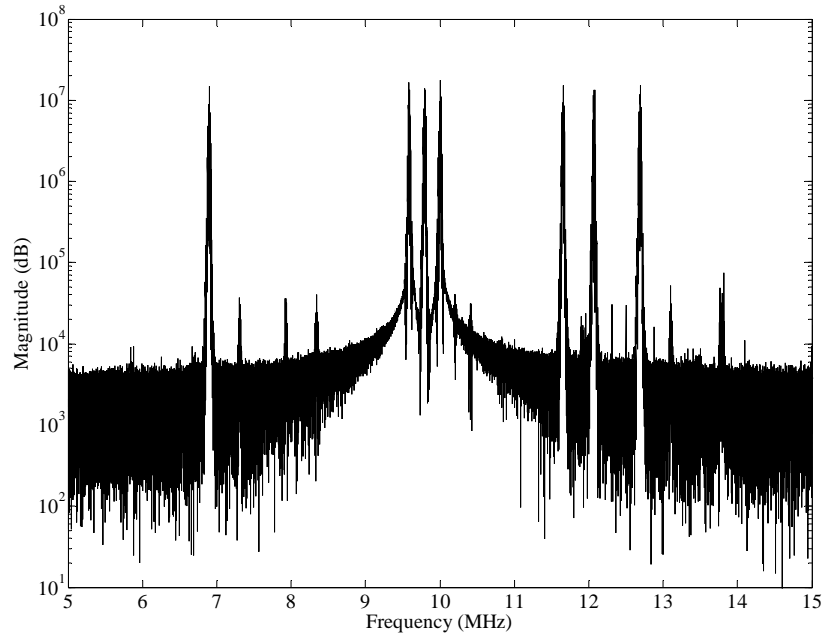Figure 2.   Instantaneous spectrum of SSB/SC modulated signal.

Figure 3.   Spectrum of a frequency-hopped MSK signal, accumulated over time [4].
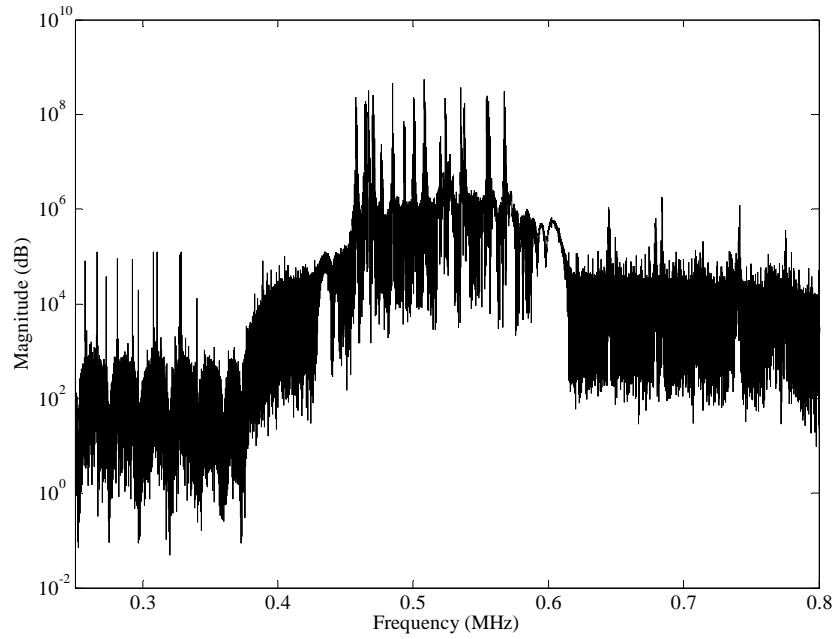

Figure 4.   Spectrum of a FH-SSB/SC signal, accumulated over time.

B. INTERFERENCE AND COMPOSITE SIGNALS

The interference waveforms used in [3] and [4] were continuous wave (CW) and binary phase-shift keyed (BPSK) signals that were generated by computer simulation. These waveforms are stationary. A collection suite was used in an urban environment to collect the interference signal. In this thesis, this signal is referred to as the field data. After collection, the field data was digitized. The field data and the laboratory data were then imported into MATLAB, added together to obtain a composite signal, and processed. Figure 5 is the power spectral density (PSD) of the field data which is used as interference. The PSD of the test signal is shown in Figure 6. As previously mentioned, the laboratory data was collected directly at the output of the transmitter and is, consequently, free of noise or any other channel impairments. The field data, on the other hand, was collected from signals transmitted in the HF band and contains a significant amount of time-varying, or non-stationary, narrow-band noise in addition to AWGN.

The laboratory data was sampled at 6.25 MHz, and the field signal was sampled at 2.5 MHz. With this sample frequency mismatch, some signal manipulation is required before the data files can be added together in order to form the composite signal.
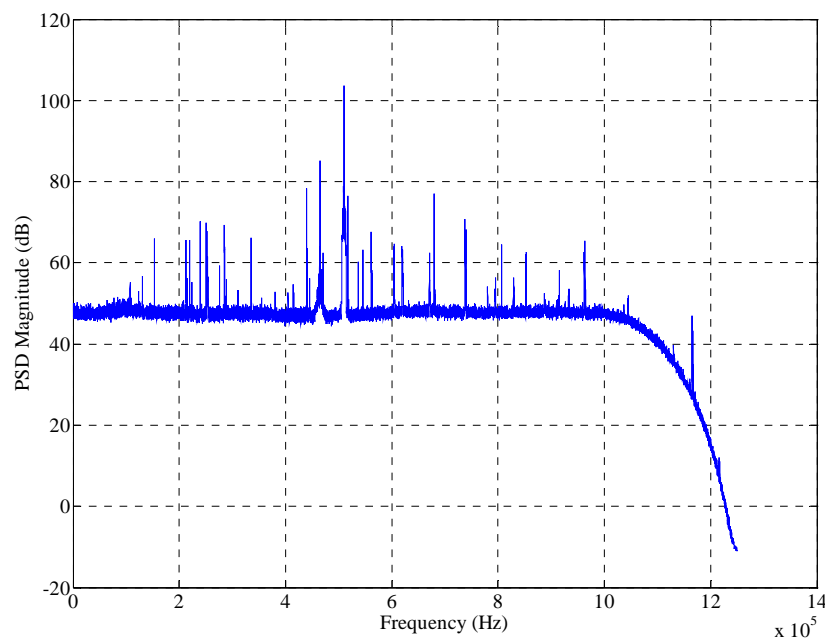

Figure 5.   PSD of non-stationary interference (field data).

6
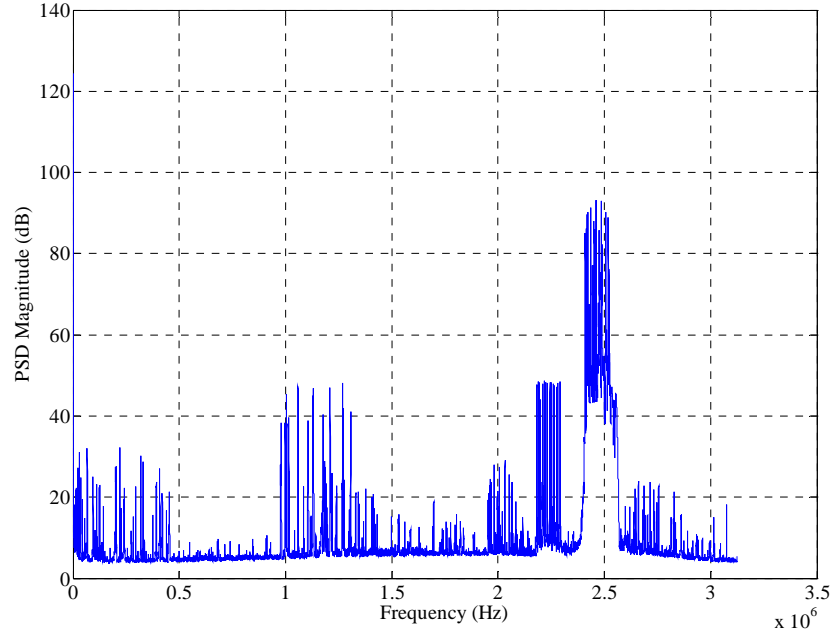
Figure 6.   PSD of HF/FH test signal without interference.

The sample frequency mismatch was resolved by first shifting the laboratory signal down to 0.5 MHz so that it is in the same bandwidth as the interference. This is accomplished by multiplying the laboratory signal by $\cos(2\pi f_c t)$, where the carrier frequency $f_c = 2.3$ MHz. The HF/FH test signal after it was shifted down to the frequency band of the interference is shown in Figure 7. Note the spectral components generated by aliasing in the 1.5 MHz to 2.5 MHz band of frequencies. The frequencies generated by aliasing were removed with a low pass filter (LPF) having a passband frequency of 0.6 MHz and a stopband frequency of 1.0 MHz. This eliminates all frequencies greater than 1.0 MHz. Finally, the frequency-shifted laboratory data is downsampled from 6.25 MHz to 2.5 MHz using the MATLAB resample command. The resample command automatically applies an anti-aliasing (lowpass) finite impulse response filter to the data being resampled. At this point, both field and laboratory signals are sampled at 2.5 MHz and each contain 16,777,216 points of data.

Figure 7.   PSD of the frequency-shifted HF/FH test signal without interference.
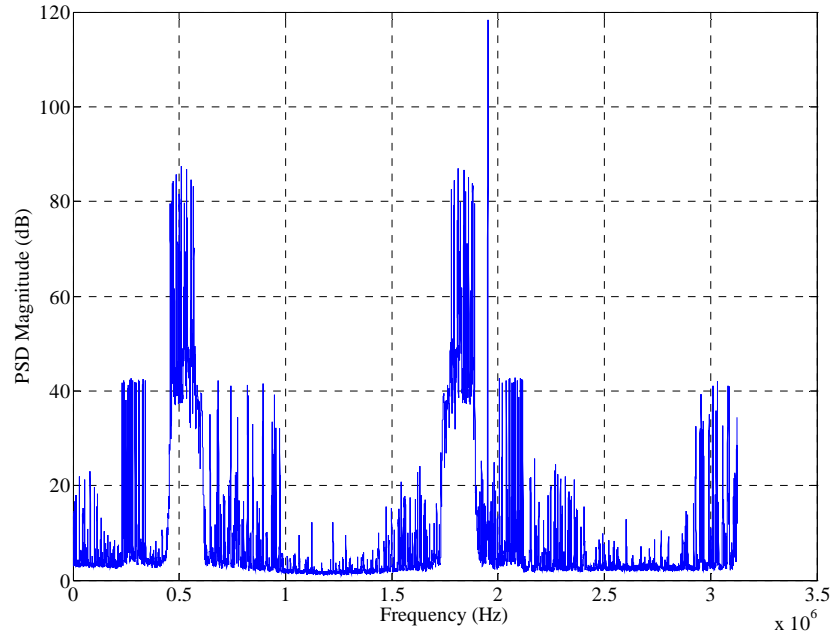
A FFT of the shifted, filtered, and downsampled version of the laboratory data is shown in Figure 8. The approximate frequency and order of each of the 16 frequency hops in the signal is shown in Table 1, and the test signal spectrum is shown in Figure 9, which is a zoomed-in version of the frequency-band in Figure 8 that contains the signal-of-interest. Note that the number of each frequency-hop as delineated in Table 1 is shown in Figure 9. A plot of the magnitude of the FFT of the non-stationary interference is shown in Figure 10. As seen in Figure 10, the spectral spikes in the interference signal could be mistaken as a frequency-hopped signal.

The HF/FH laboratory signal and the non-stationary data (field data) were added together, and the magnitude of the FFT of the composite signal is shown in Figure 11. The frequency-hopped signal is difficult to recover from the composite waveform using filter-based detection methods due to the fact that the signal-of-interest is now obscured by an overwhelming amount of interference. This can be seen in Figure 12, where hops 2, 4, 6, 10, and 12 are competing with interference at the same frequency.
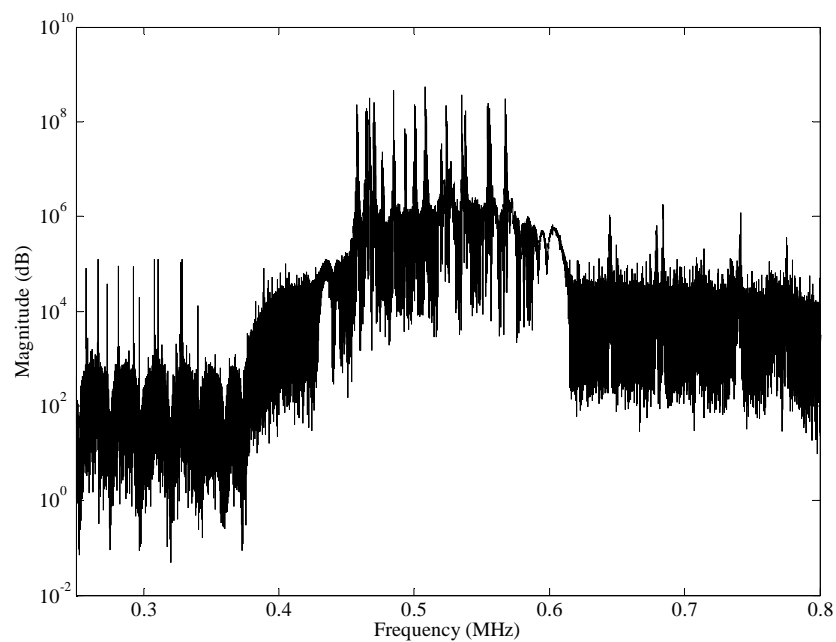
Figure 8.   Fourier transform of shifted, filtered, and downsampled laboratory data.
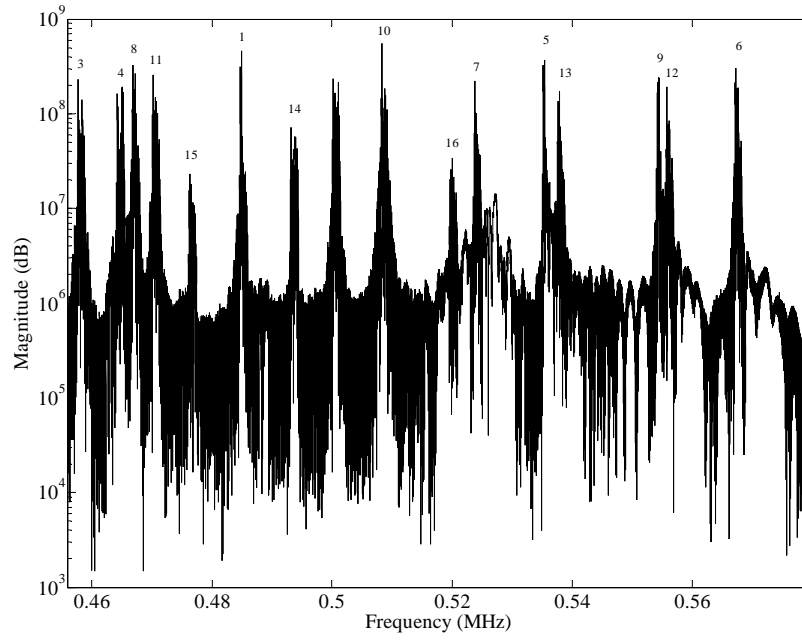
Figure 9.   Zoomed-in version of Figure 8.

Table 1.   Frequencies and sequence order of hops in frequency-shifted, filtered, and downsampled laboratory data.

Approximate Carrier Frequency of Hop	Hop Number	Approximate Carrier Frequency of Hop	Hop Number
0.4577 MHz	3	0.5083 MHz	10
0.4650 MHz	4	0.5201 MHz	16
0.4672 MHz	8	0.5238 MHz	7
0.4702 MHz	11	0.5354 MHz	5
0.4763 MHz	15	0.538 MHz	13
0.4849 MHz	1	0.5545 MHz	9
0.4939 MHz	14	0.5562 MHz	12
0.5002 MHz	2	0.5673 MHz	6
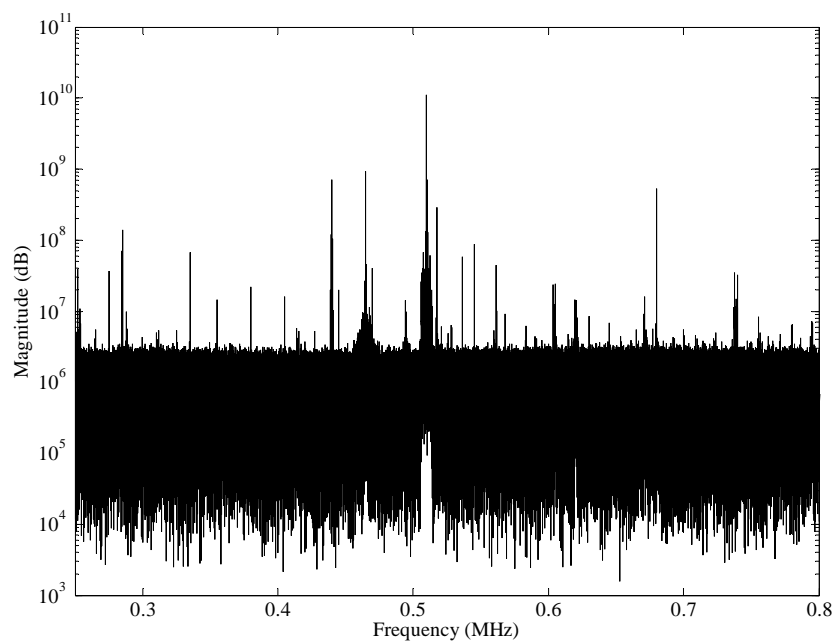
Figure 10.   Fourier transform of non-stationary interference (field data).
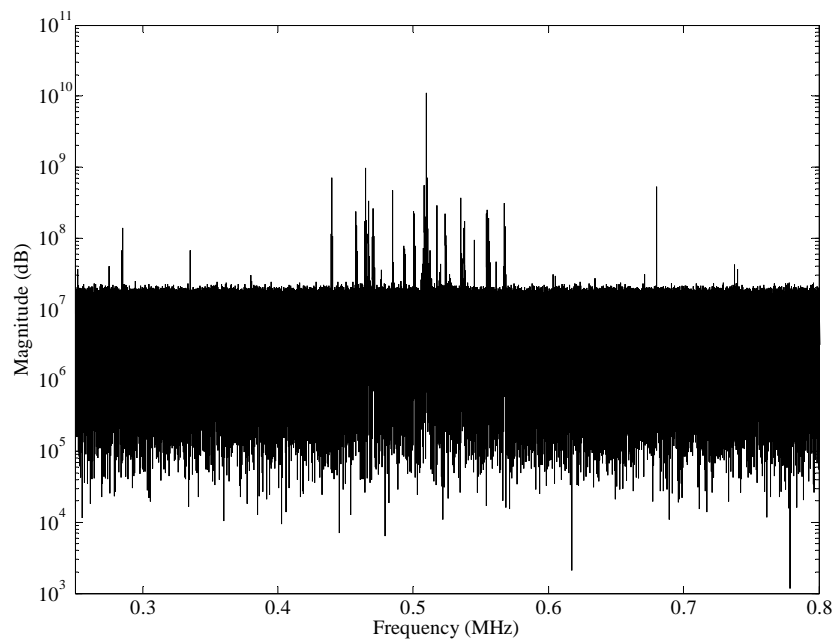
Figure 11.   Fourier transform (magnitude) of the composite signal.
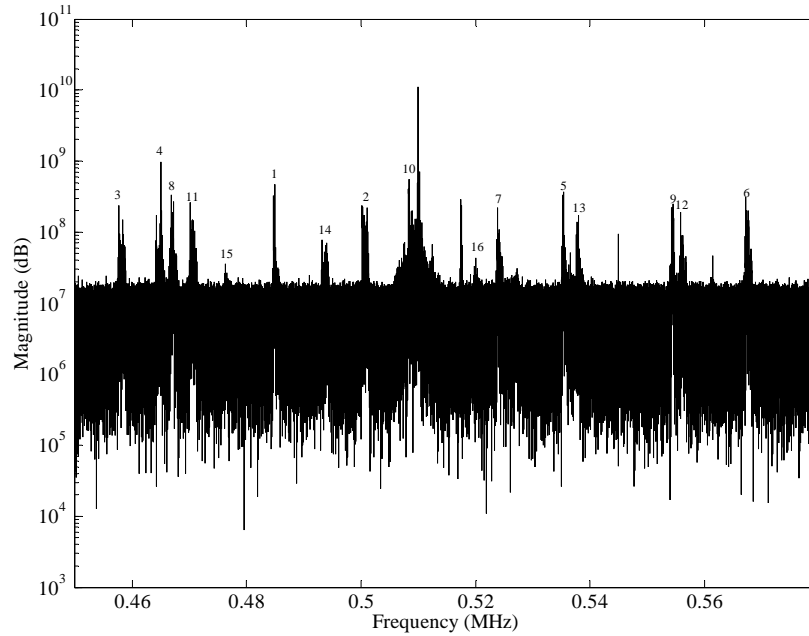
Figure 12.   Zoomed-in version of Figure 11.

This chapter gave the reader an understanding of the signals used in this thesis and the required manipulation of the HF/FH laboratory data in order to properly embed it in the field data used as interference. This composite waveform is the composite signal that is analyzed in the following chapters. The next chapter builds on previous work in [3] and [4] to use an exponential averaging algorithm to form an estimate of non-stationary interference signal which is then used to recover the signal-of-interest embedded in the interference.

III. HF/FH SIGNAL RECOVERY USING EXPONENTIAL AVERAGING

The exponential averaging algorithm presented in [3] and [4] is applied to real-world data in this chapter. Specifically, the detection of the presence of the HF/FH test signal embedded in non-stationary interference signals, AWGN, and received in a real-world environment is investigated. The steps taken to recover the HF/FH signal, such as interference estimation and recovery using spectral subtraction or division, will be discussed.

A.   INTERFERENCE ESTIMATION

The first step in recovering the FH signal that is embedded in interference is to determine the frequency-domain representation of the interference signal by exponentially averaging many short FFTs of the composite signal over time. The composite HF/FH signal plus the interference it was embedded in was broken into smaller data segments (*N*-point windows), and the magnitude of the FFT of each *N*-point window was computed. These window FFTs were then used to form the interference estimate which ideally has none of the HF/FH signal remaining. A block diagram of the spectral interference estimate is shown in Figure 13 and is expressed mathematically as

$$X(i) = \sum_{k=0}^{L-1} \beta^k M_k(i),\qquad(1)$$

where *X(i)* is the spectral interference estimate, β is a weight factor between 0 and 1, $M_k(i)$ is magnitude squared of the FFT of the current *N*-point window, and $k = 0,1,2,\ldots,L-1$ where $L = 16{,}777{,}216/N$ is the number *N*-point of segments that the data is separated into. The parameters β and *N* are determined by trial and error which will be explained later in this chapter. A block diagram of the spectral interference estimate is shown in Figure 13.
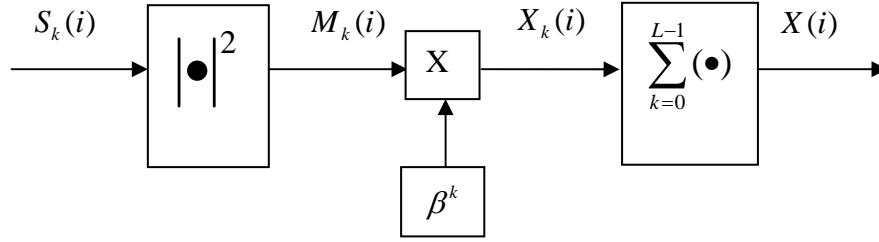
Figure 13.   Exponential averaging interference estimate block diagram.

where $S_k(i)$ is the FFT of one N-point data block,

Determination of the parameters β and N is a key step in obtaining an interference estimate. The following discussion may seem to infer that β and N are obtained sequentially and independently, but in reality they are obtained in conjunction with one another. In the discussion of the determination of N, the best β is assumed; although, in practice the best N and the best β must be found by varying both parameters.

The parameter N determines the number of frames (FFT length) and the resolution of the estimate. As can be seen by comparing Figure 10 with the interference estimate in Figure 14, obtained with $N = 2^{12}$, the interference is not accurately estimated. Comparing Figure 10, Figure 11, and Figure 15, we see that $N = 2^{20}$ gives a better estimate of the interference but does not extract the HF/FH signal. This is due to the fact that a large FFT window results in an estimate based on a small number of windows and does not average out all the frequency-hop components. From trial-and-error, a window size of $N = 2^{16}$ produced the best interference estimate while simultaneously suppressing the HF/FH signal. The result is shown in Figure 16. A window size of $N = 2^{16}$ is used for the remainder of this thesis.
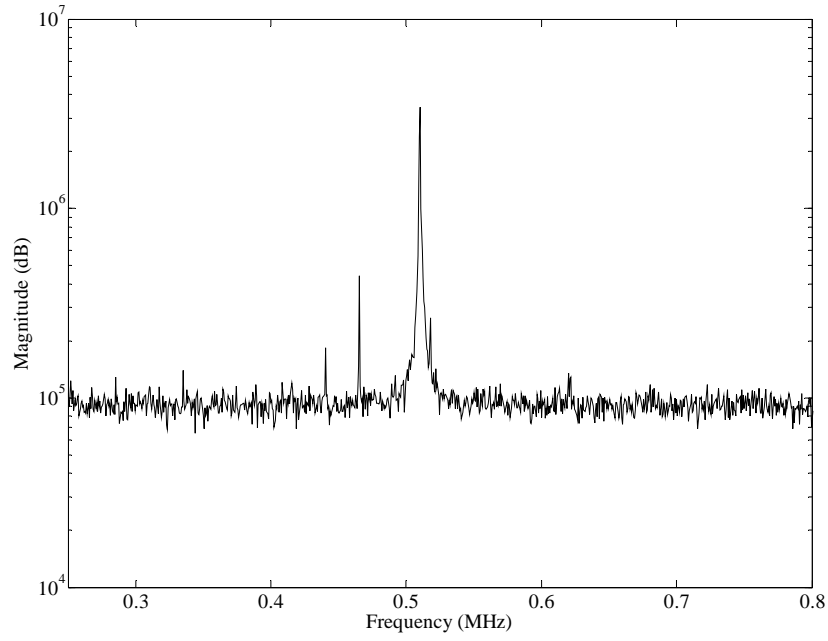
Figure 14.   Spectral estimate of the interference using a $N = 2^{12}$ point FFT with $\beta = 0.93$.

Figure 15.   Spectral estimate of the interference using a $N = 2^{20}$ point FFT with $\beta = 0.93$.

15

Figure 16. Spectral estimate of the interference using a $N = 2^{16}$ point FFT with $\beta = 0.93$.

From [3] the FFT window used to form an interference estimate must meet the requirement

$$\frac{N}{F_s} \leq T_{hop}, \tag{2}$$

where F_s is the sample rate, T_{hop} is the duration of a frequency hop, and N is the FFT window size.

The constraints given by (2) are tested for $N = 2^{16}$ to ensure that (2) is satisfied. For a sample rate of 2.5 MHz, the sampling period is

$$T_s = \frac{1}{F_s} = \frac{1}{2.5 \times 10^6} = 0.4 \ \mu s. \tag{3}$$

For a frame length of 2^{16}, the window duration is

$$T_w = (2^{16} \text{ samples})(0.4 \ \mu s) = 26.21 \text{ ms}. \tag{4}$$

A hop rate of 5.0 hops/s implies $T_{Hop} = 0.2$ s/hop. Hence, we see that a window size of 2^{16} satisfies the limits set by (2) since

$$26.21 \text{ ms} < 0.2 \text{ s.} \tag{5}$$

Another important parameter in the exponential averaging algorithm is the weight factor β, where $0 \le \beta \le 1$. The weight factor defines how much earlier elements in the exponential average contribute to the interference estimate [4]. A large weight factor results in over emphasizing early-time hops. As a result, the contribution of early-time hops in the sequence does not diminish rapidly because each new frame only contributes a small amount to the estimate. As seen in Figure 17, when a large weight factor is used, the HF/FH signal is not completely extracted from the interference estimate. This can be seen by comparing Figure 17 with Figure 10, the FFT of just the interference, and Figure 11, the FFT of the composite signal. Clearly, a significant part of the FH signal is still present in Figure 17. The frequency hops that are easily discriminated in Figure 17 are indicated using the numbers from Table 2. A small weight factor results in over-emphasizing the contribution of late hops in the time sequence. In Figure 18, it is seen that a small weight factor does not give a good representation of the interference when compared to Figure 10 because some of the interference components are suppressed. As can be seen in Figure 19, a weight factor of $\beta = 0.93$ yields the balance needed to best represent the interference estimate and is the weight factor used from this point on in this thesis.
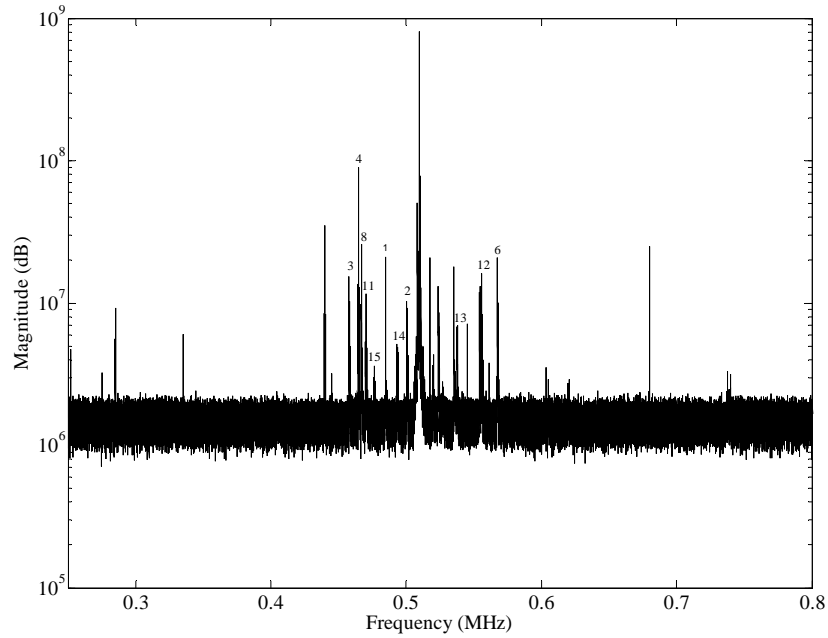
Figure 17.   Spectral estimate of the interference using a $N = 2^{16}$ point FFT with $\beta = 0.99$.

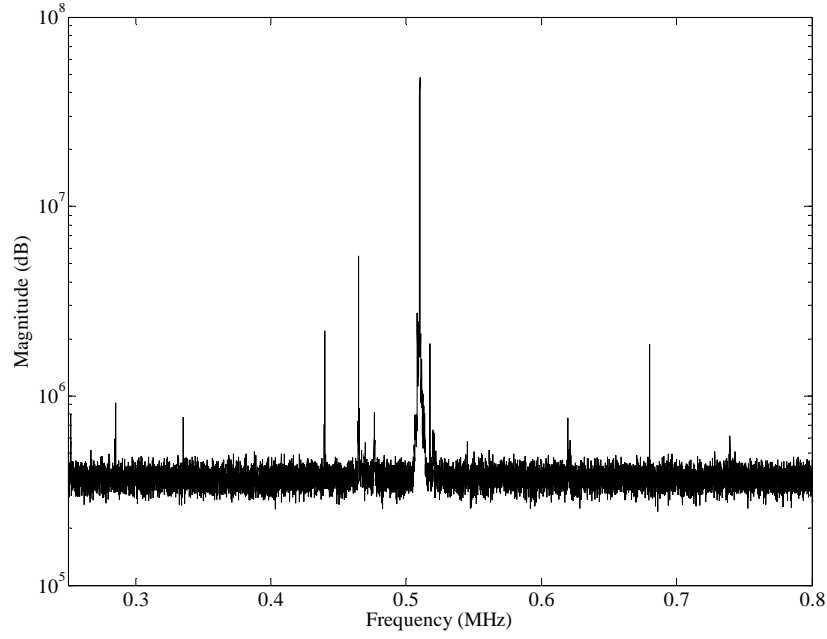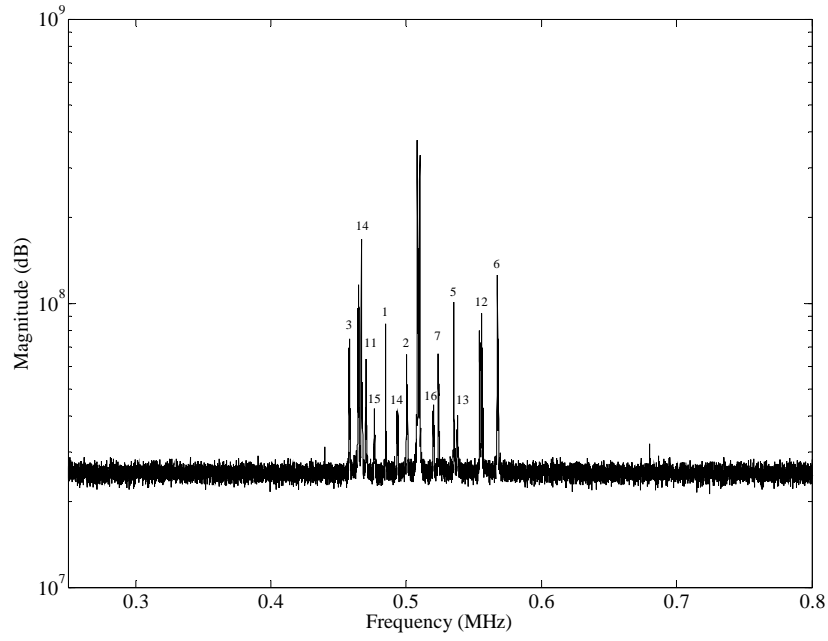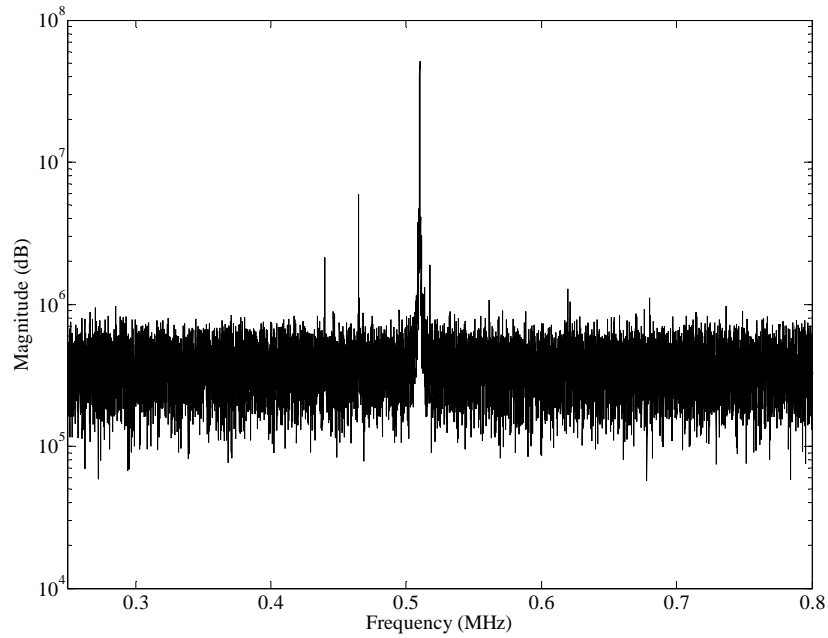Figure 18.   Spectral estimate of the interference using a $N = 2^{16}$ Point FFT with $\beta = 0.35$.
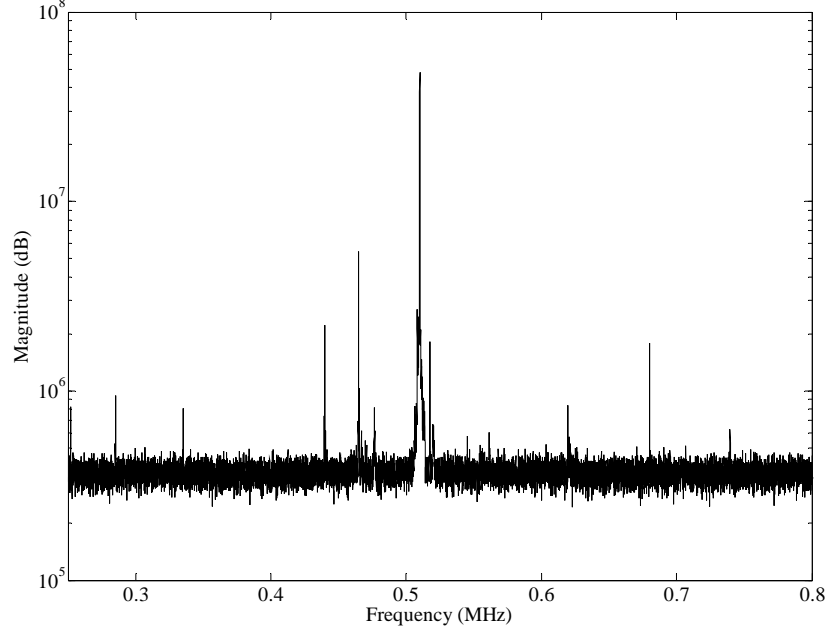
Figure 19.   Spectral estimate of the interference using a $N = 2^{16}$ point FFT with
$$\beta = 0.93.$$

B.   HF/FH SIGNAL SPECTRUM ESTIMATION

Now that an acceptable interference estimate has been obtained, the HF/FH signal is recovered using methods developed in [4]. The two approaches used to recover the frequency-hopped signal are spectral subtraction and spectral division. The data used in this thesis are tested using both methods.

Frame-by-frame division of the HF/FH signal by the interference estimate is expressed analytically as

$$\bar{Y}_{FH}(i) = \sum_{k=1}^{L-1} \frac{M_k(i)}{X(i)}, \qquad (6)$$

where $\bar{Y}_{FH}(i)$ is the estimate of the HF/FH signal, $M_k(i)$ is the magnitude squared of the FFT of the current window in the signal and $X(i)$ is the previously obtained spectral interference estimate.

Frame-by-frame subtraction of the HF/FH signal by the interference estimate expressed analytically as

$$\overline{Y}_{FH}(i) = \sum_{k=1}^{L-1} M_K(i) - \alpha X(i), \tag{7}$$

where α is an element-by-element scaling factor used to normalize $X(i)$ with respect to $M_k(i)$ and is essentially the ratio of the interference estimate to the actual interference data. A technique to determine the scaling factor from the data is given in [4]. The scaling factor ensures that the magnitude of the spectrum of the interference estimate and the magnitude of the spectrum of the data representing the composite signal are the same. If there is a significant magnitude mismatch, the subtraction technique does not work well.

The results obtained using spectral divisions are shown in Figures 20 through 22 for different values of β. The FFT window size N and weight factor β that are used to obtain the interference estimate affects signal estimation by spectral division as well. As seen in Figure 20, a large weight factor does not eliminate all the interference components, and a small weight factor increases the noise variance, as seen in Figure 21. After several iterations, it was determined that $\beta = 0.93$ yields the balance needed to allow the contributions from individual hops to be as uniform as possible. This can be seen in Figure 22. A similar evaluation of the effects of β and N on signal estimation using spectral subtraction were also done, but only the results for the combinations of β and N providing the best signal recovery are shown in Figure 23.

The recovered signal frequency-hops are shown in Figure 22 for spectral division and in Figure 23 for spectral subtraction. As can be seen, in this zero AWGN, high SIR case, spectral subtraction is superior to spectral division in terms of number of frequency hops recovered.
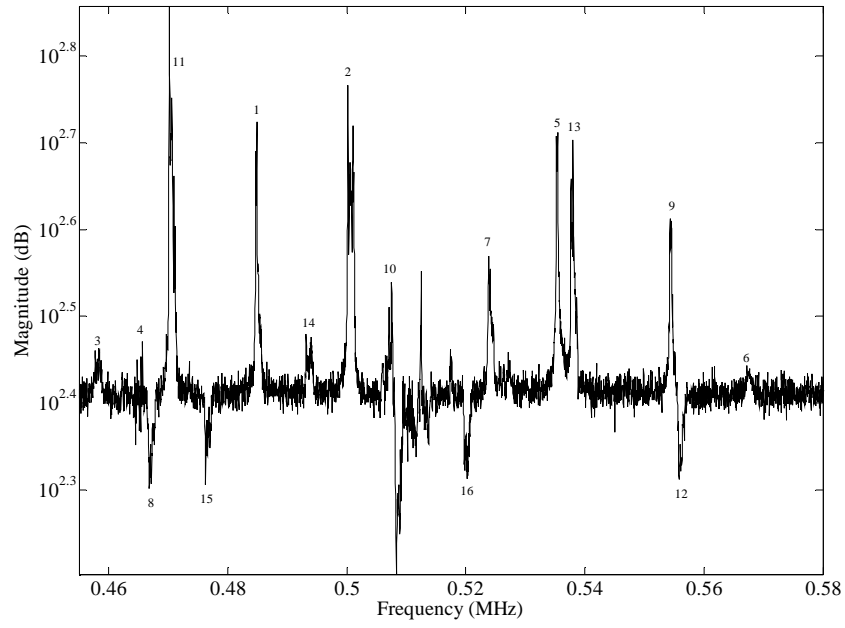
Figure 20.   Spectral estimate of the HF/FH signal using division, $\beta = 0.96$.
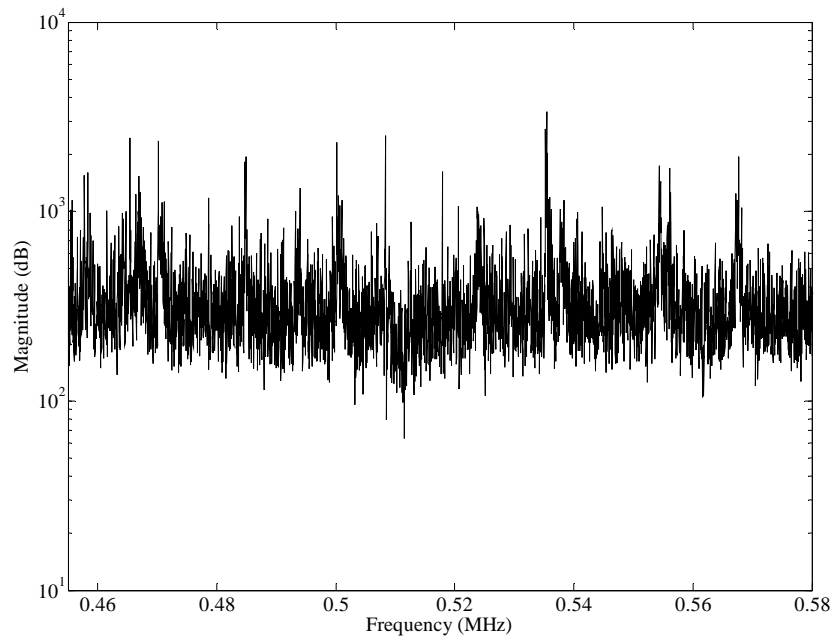

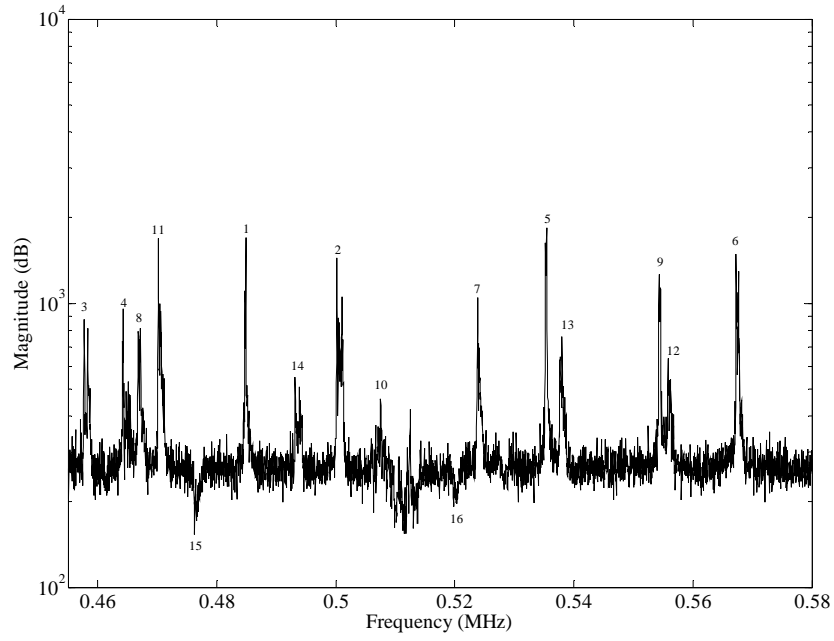Figure 21.   Spectral estimate of the HF/FH signal using division, $\beta = 0.35$.

21

Figure 22.   Spectral estimate of the HF/FH signal using division, $\beta = 0.93$.
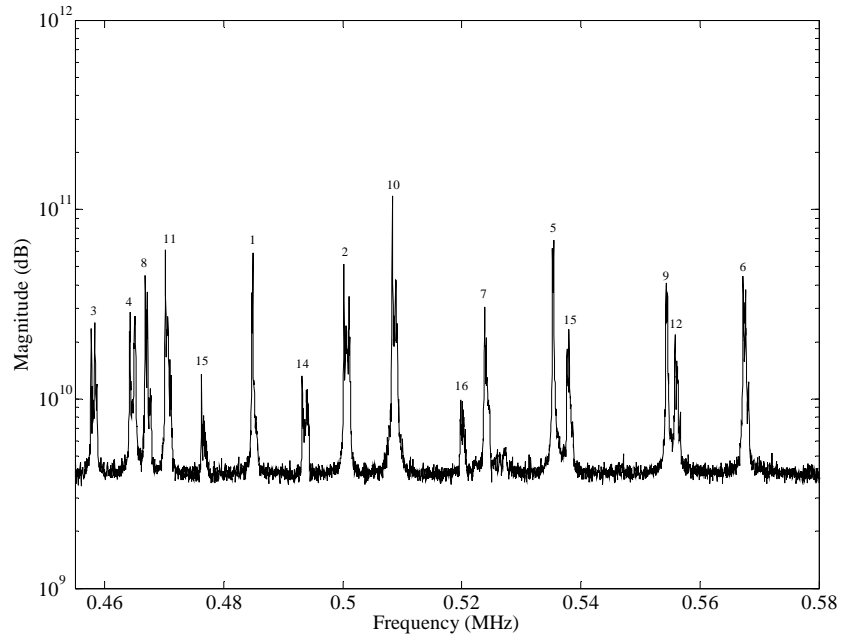
Figure 23.   Spectral estimate of the HF/FH signal using subtraction, $\beta = 0.93$.

C.   CHAPTER SUMMARY

A recovery method for the HF/FH signal was discussed in this chapter. It was shown that choosing the correct FFT window size N and weight factor β are critical for effective detection. With a window size of $N = 2^{16}$ points and a weight factor of $\beta = 0.93$, an accurate interference estimate and an accurate estimate of the HF/FH signal is obtained. From previous work, the last hops in the sequence may not be recovered by spectral division. In this case, hop numbers 5 and 10 are not recovered by spectral division, but these correspond to the lowest energy hops in the test signal, as can be seen in Figure 9. Spectral subtraction, on the other hand, recovers all of the frequency hops in the signal. The effects of AWGN and the signal-to-interference ratio on signal estimation are examined in the next chapter.

THIS PAGE INTENTIONALLY LEFT BLANK

IV. EFFECT OF SIGNAL-TO-INTERFERENCE AND SIGNAL-TO-NOISE RATIOS

The purpose of this chapter is to analyze the effects different SIR and SNR combinations have on interception and detection of the HF/FH signal. Both spectral division and spectral subtraction are considered in this section.

The signal-to-interference was normalized by first computing

$$SIR = \frac{\sum_{0}^{N-1}\left|FFT_{HF/FH}\right|^2}{\sum_{0}^{N-1}\left|FFT_I\right|^2} \quad , \tag{8}$$

where $FFT_{HF/FH}$ is the fast Fourier transform of the HF/FH test signal, and FFT_I is the fast Fourier transform of the interference signal. The numerator and denominator individually define the power of the HF/FH test signal and the interference signal, respectively, using Parseval's theorem [6]. The ratio is the SIR. Next, the inverse of (8) and the HF/FH test signal were multiplied to normalize the SIR to unity. Now the test signal data can be manipulated to represent a range of SIR. In addition, AWGN is also taken into account by combining AWGN with the HF/FH test signal using the MATLAB function

$$Y = \text{awgn}\ (X, \text{SNR}, \text{'measured'}), \tag{9}$$

where X is the HF/FH test signal, SNR the specific signal-to-noise ratio per sample in dB, and 'measured' implies that the power of the HF/FH test signal is measured before adding AWGN.

The following discussion of Figures 24 through 32 pertains to signal estimation using spectral division, and the primary results are summarized in Table 2. A similar examination was performed for spectral subtraction, but the details for spectral subtraction are not shown. Instead, they are summarized in Table 3.

The results for spectral division when SIR = 0 dB and there is no AWGN is shown in Figure 24. Several SIR and SNR combinations are used to determine the effects of each on detection and processing. In Figure 25 and Figure 26, no AWGN was introduced to the signal-of-interest and the SIR was varied. In Figure 28 and Figure 28, the SIR was held constant and different power levels of AWGN were introduced. Figure 29 is a combination of decreasing the SIR and adding AWGN to the HF/FH signal. As expected, as the SIR decreases and the AWGN power increases, the number of detectable frequency-hops decreases.

Figure 24.   Spectral division estimate of the HF/FH signal, SIR = 0 dB, no AWGN.

Figure 25.   Spectral division estimate of the HF/FH signal, SIR = −10 dB, no AWGN.
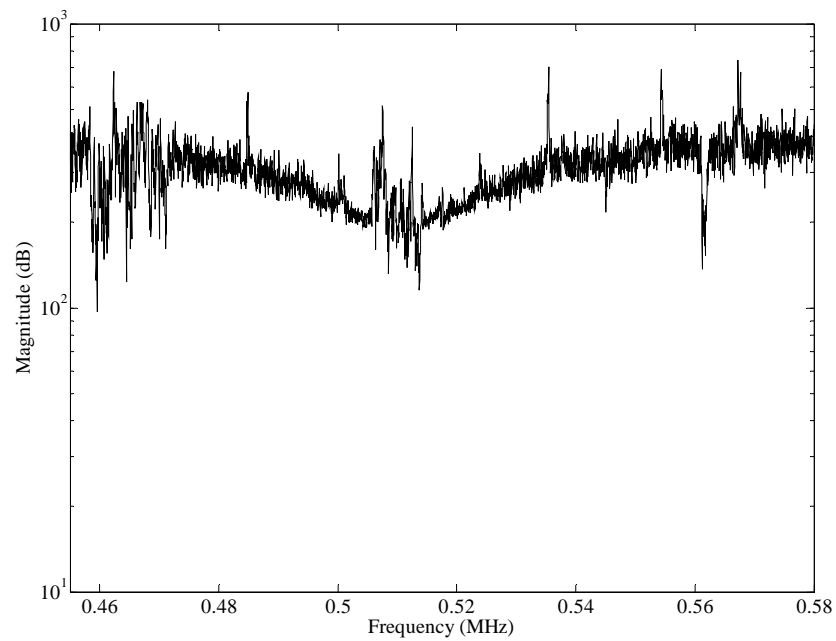
Figure 26.   Spectral division estimate of the HF/FH signal, SIR = −16 dB, no AWGN.
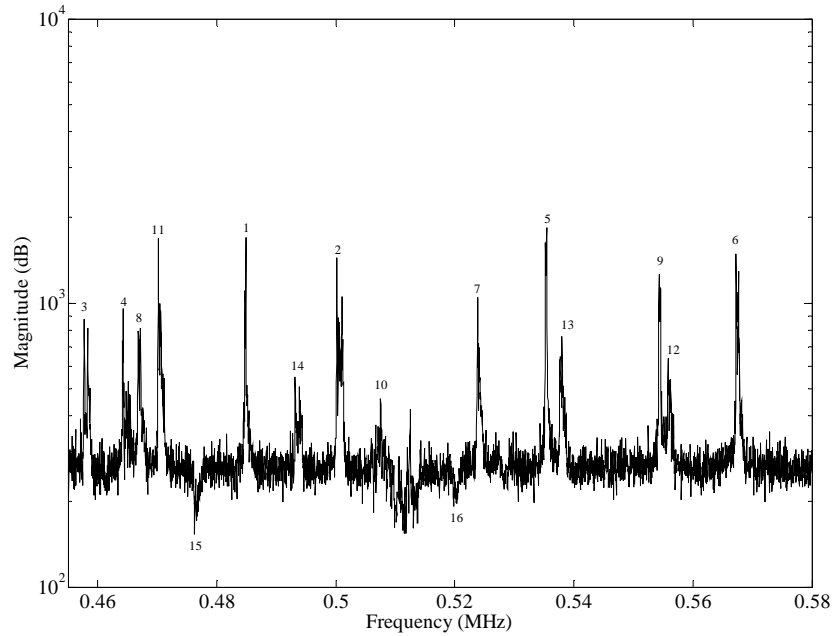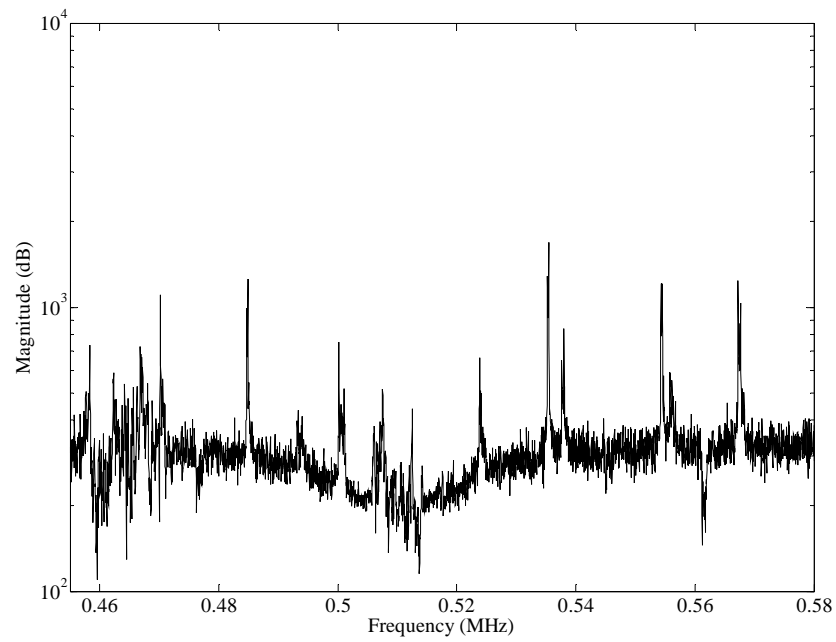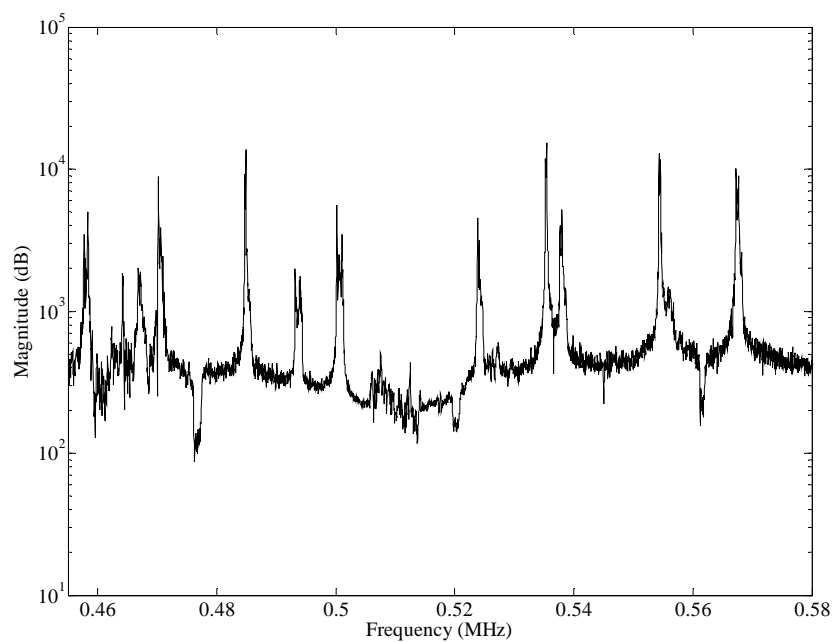
Figure 27.   Spectral division estimate of the HF/FH signal, SIR = 0 dB, SNR=30 dB.
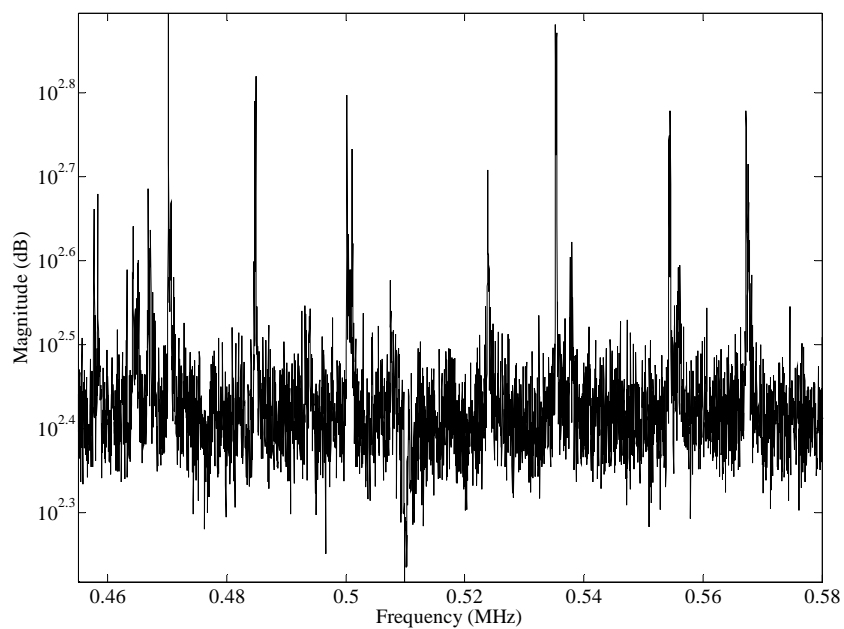
Figure 28.   Spectral division estimate of the HF/FH signal, SIR = 0 dB, SNR = −10 dB.
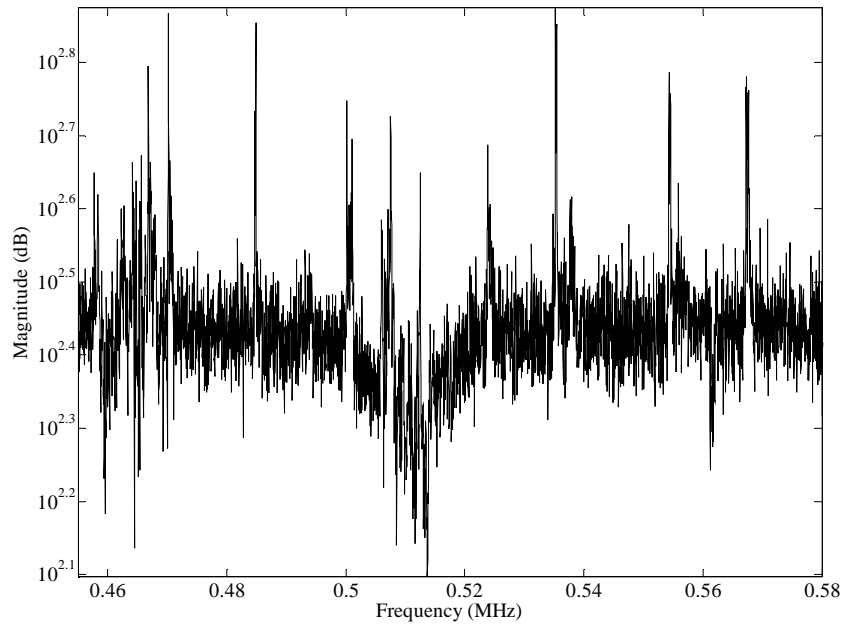
Figure 29.   Spectral division estimate of the HF/FH signal, SIR= −10 dB, SNR = −10 dB.

Figure 30, Figure 31, and Figure 32 show how different SNRs and SIRs affect the total received signal. As the SNR decreases, the noise floor increases and begins to engulf the total received signal. The combination of decreasing the SNR and SIR causes the HF/FH test signal to be completely engulfed in the interference, as can be seen in Figure 32.
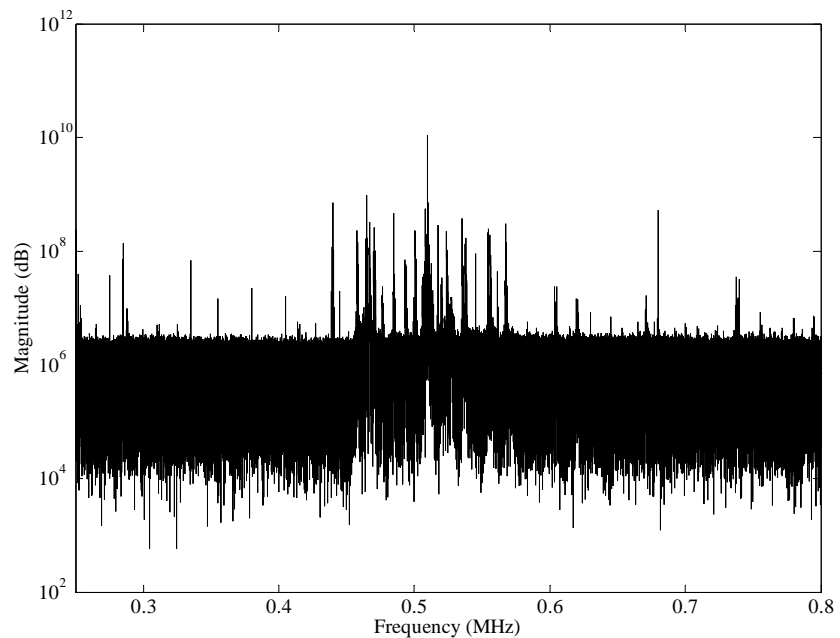
Figure 30. Frequency domain representation of the total received signal, SIR = 0 dB,

SNR = 30 dB.
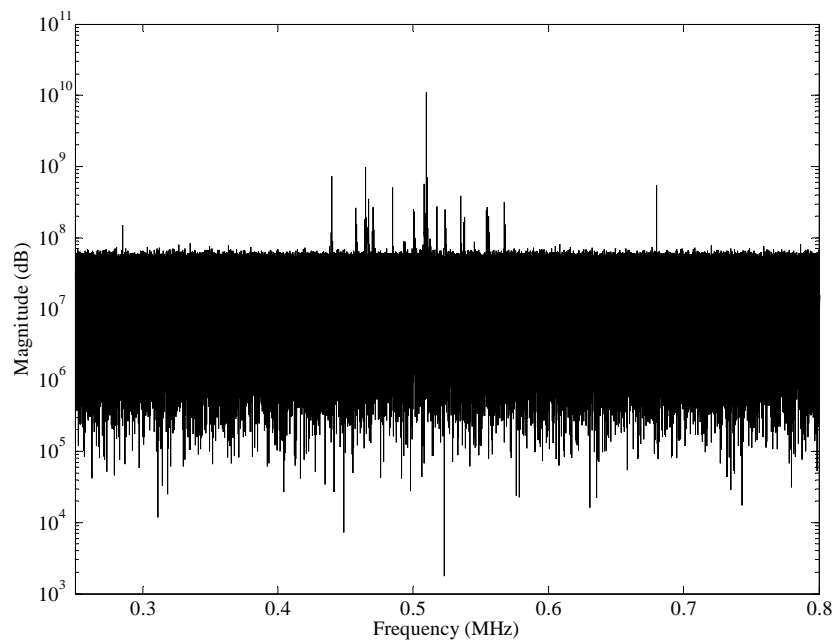
Figure 31. Frequency domain representation of the total received signal, SIR = 0 dB,

SNR = −10 dB.

30
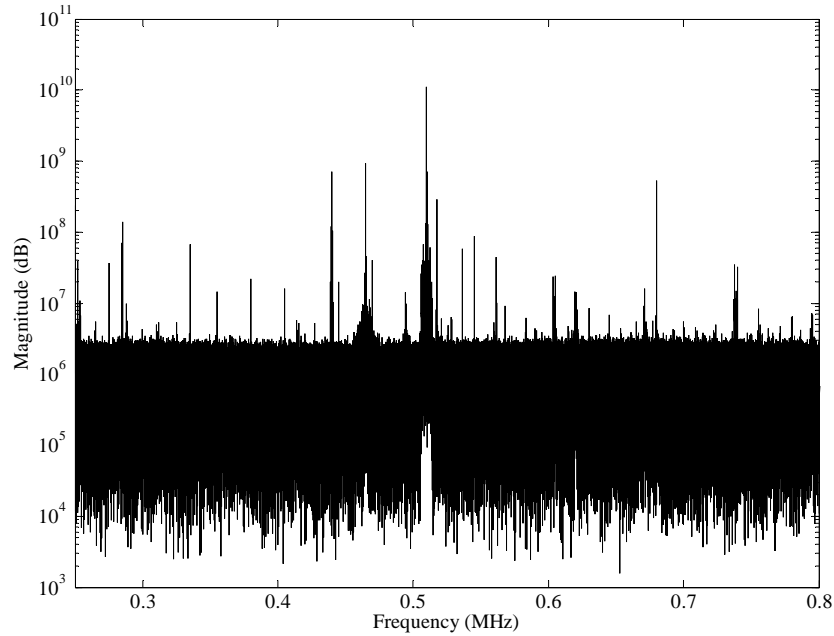
Figure 32.   Frequency domain representation of the total received signal, SIR = −10 dB, SNR = −10 dB.

The exponential averaging algorithm was run using 50 different combinations of SNR and SIR for spectral division and 25 different combinations of SNR and SIR for spectral subtraction. The results are presented in Tables 2 and 3. The yellow cells represent the combinations of SNR and SIR that result in successful processing of the HF/FH test signal, and the blue cells represent the combinations of SNR and SIR that result in successful detection of the HF/FH test signal. It is assumed that successful processing is when all but two frequency-hops are recovered, and successful detection is when at least half of the frequency-hops are recovered. As can be seen, spectral subtraction is superior when the SIR is large, but spectral division performs better when SIR is smaller. When SIR is large enough for spectral subtraction to be effective, reducing SNR has more effect on spectral division than on spectral subtraction.

Table 2.   The number of frequency hops detected by spectral division given a HF/FH signal in the presence of AWGN and interference.

SNR dB (across) SIR dB (down)	No AWGN	−4	−8	−10	−12
0	14	14	12	10	9
−2	14	14	12	10	9
−4	14	14	12	10	9
−8	13	13	11	9	8
−10	10	10	9	8	8
−12	8	8	7	5	2
−14	5	5	4	3	1
−16	3	3	3	2	0
−18	2	1	0	0	0
−20	0	0	0	0	0

Table 3.   The number of frequency hops detected by spectral subtraction given a HF/FH signal in the presence of AWGN and interference.

SNR dB (across) SIR dB (down)	No AWGN	−4	−8	−10	−12
0	16	16	16	12	11
−2	14	14	14	10	9
−4	10	10	8	5	4
−8	5	5	4	3	1
−10	0	0	0	0	0

The thresholds of detection and processing of the HF/FH test signal as a function of SIR and SNR were developed in this section. In the next and final chapter of this thesis, the results presented in the previous chapters on the detection of the HF/FH test signal embedded in real-world non-stationary interference are summarized.

V.   CONCLUSIONS

A.   CONCLUSIONS

The recovery of a signal generated by a HF/FH test signal when the signal was embedded in real-world, non-stationary interference was the subject of this thesis. An estimate of the interference spectrum was created by applying an exponential averaging algorithm to frames of the composite signal plus interference data. The number of frames used in each estimate, the weight applied to each frame, and FFT size are the variables involved in generating the interference estimate. For a 16,777,216-point data set, a FFT window of $N = 2^{16}$ and a weight factor β of 0.93 produced a good interference spectrum estimate. After the interference estimate is determined, it is used to normalize the total received signal which results in the recovery of the HF/FH signal. Spectral subtraction provides the best HF/FH signal estimate at high SNR and SIR, but as SNR and SIR decrease, spectral division outperforms spectral subtraction. In spectral subtraction the total received signal is subtracted frame-by-frame by a scaled version of the interference estimate, and in spectral division the total received signal is divided frame-by-frame by the interference estimate. The spectral picture of the recovered HF/FH signal is produced by summing all the normalized frames together. The threshold of detection and processing were determined for a combination of different signal-to-noise and signal-to-interference ratios. It was assumed that recovery of $n - 2$ frequency hops of an n-hop signal imply that this signal can be processed and $n/2$ recovered hops imply that the signal can be detected. For spectral division, a SIR of −4 dB and a SNR of −4 dB were determined to be the threshold for processing, and a SIR of −12 dB and a SNR of −4 dB were found to be the threshold for detection. For spectral subtraction, a SIR of −2 dB and a SNR of −8 dB were determined to be the threshold for processing, and a SIR of −4 dB and a SNR of −8 dB were found to be the threshold for detection.

B.   FUTURE WORK

Recommendations for future work in detection and processing of frequency-hopped signals are briefly presented in this section. One future research area would be to use the composite frequency-hop signal and non-stationary interference signal collected

in the same data set to recover the signal-of-interest using the methods discussed in this thesis. Another future research topic would be to take the work in this thesis a step further and not only expose the frequency-hop signal to non-stationary interference but also to non-stationary AWGN.

LIST OF REFERENCES

[1]   R.L. Peterson, R.E. Ziemer, and D.E. Borth, *Introduction to Spread Spectrum Communications*, Prentice Hall, Upper Saddle River, NJ, 1995.

[2]   J.G. Proakis, *Digital Communications*, 4th ed., McGraw Hill, New York, NY, 2001.

[3]   Christopher Brown, Kyle Kowalske, and Clark Robertson, "Detection of frequency-hopped waveforms embedded in interference waveforms," *Proc. IEEE Military Communications Conference,* vol. 2, pp. 747-753, 2005.

[4]   John Webber, Kyle Kowalske, Clark Robertson, Frank Kragh, and Christopher Brown, "Detection of frequency-hopped waveforms embedded in interference Waveforms with Noise," *Proc. Of IEEE   International Communications Conference,* 2007.

[5]   Clark Robertson, Notes for EC3510 Communications Engineering, Naval Postgraduate   School, Monterey, CA, 2007.

[6]   Leon W. Couch II, *Digital and Analog communication systems,* 5th ed., Printice Hall, 1997.

THIS PAGE INTENTIONALLY LEFT BLANK

INITIAL DISTRIBUTION LIST

1.   Defense Technical Information Center
      Ft. Belvoir, Virginia

2.   Dudley Knox Library
      Naval Postgraduate School
      Monterey, California

3.   Chairman, Code EC
      Department of Electrical and Computer Engineering
      Naval Postgraduate School
      Monterey, California

4.   Professor R. Clark Robertson, Code EC/Rc
      Department of Electrical and Computer Engineering
      Naval Postgraduate School
      Monterey, California

5.   Professor Roberto Cristi, Code EC/Cr
      Department of Electrical and Computer Engineering
      Naval Postgraduate School
      Monterey, California

6.   LT Steven C. Layfield
      United States Navy
      Suitland, Maryland